Analysis and statistical interpretation of biaxial material constants derived according to EN 17117-1:2018

Van Craenenbroeck, Maarten; Mollaert, Marijke; De Laet, Lars

Published in:
Composite Structures

DOI:
10.1016/j.compstruct.2020.113235

Publication date:
2021

Analysis and statistical interpretation of biaxial material constants derived according to EN 17117-1:2018

Maarten Van Craenenbroeck[a,*], Marijke Mollaert[a], Lars De Laet[a]

[a] *Architectural Engineering, Vrije Universiteit Brussel, Pleinlaan 2, 1050 Brussel, Belgium*

Abstract

Utilising fabrics as an engineering material allows for the creation of lightweight structures, but poses some challenges when it comes to deriving material properties for use in numerical models due to the complex composite-like nature of these coated fabrics.

Until recently, no international standard regarding testing these materials and deriving their material properties existed. With the publication of EN 17117-1:2018, guidelines to biaxially test fabrics and derive material constants are now available.

To evaluate the methodology presented in EN 17117-1:2018 an analysis of the test results was carried out. A statistical interpretation allowed for the evaluation of the data variability while verifying the feasibility of a stochastic approach describing the derived material constants. This latter could be a valuable addition in e.g. reliability analyses.

Results obtained from ten tests utilising the methodology suggested in EN 17117-1:2018 are discussed and evaluated. Next, a method to verify and evaluate the statistical properties of the derived constants is proposed.

The obtained stress-strain results and material constants indicate a good consistency between the conducted tests. The process of applying statistical distributions showed to be relatively straightforward and yields compatible

*Corresponding author
Email address: maarten.van.craenenbroeck@vub.be (Maarten Van Craenenbroeck)

distributions describing the data. However, some limitations, mostly related to the sample size, still exist.

Keywords: biaxial testing, coated fabrics, linear elastic orthotropic, EN 17117-1, statistical distributions, material characterisation

1. Introduction

Tensile fabric structures invoke a combination of material prestress and clever geometric design to turn lightweight and flexible coated textiles into strong and stable structures. Utilising a material with such a low selfweight, yet a relatively high strength, allows for the building of structures with a large free span and a considerable load bearing capacity.

Due to their unique nature, designing and building fabric structures requires experience and expertise. Most of this comes down to utilising a textile as an engineering material and the unique challenges it poses to the designer. Temporal effects, such as creep and relaxation, the highly anisotropic behaviour of the woven material, the inherently large displacements due to a high material flexibility, etc. should all be taken into account during the design process to ensure the structure can be considered "safe" during its lifetime. [1, 2]

The coated woven textiles that are used within these structures present us with a very specific mechanical behaviour due to their composite-like composition. As the plastic-coated weave is typically asymmetric, consisting of two main orthogonal directions called warp and weft, the strain response under load is nonlinear and dependent on the direction. Applying a load at an angle to either of these main fibre directions leads to a very low material strength and stiffness. In addition do the two fibre directions interact strongly with each other (= "crimp interchange"), making the material's behaviour also dependent on the applied load ratio. Overall, fabrics present engineers with a nonlinear anisotropic behaviour, making modelling the material behaviour accurately challenging and still subject to ongoing research. [3, 4, 5]

While the establishment of numerical models is important to allow engineers

to simulate the textile's material behaviour in depth, these models still require experimental input data regarding the material's response under loading. Up until recently a standardised test procedure for coated textiles did however not exist, resulting in the utilisation of different test approaches which can yield a considerable variation on the material parameters derived from these different tests [6, 7, 8]. This, together with the natural variation that exists within a woven material as a consequence of, amongst others, the manufacturing process and intrinsic imperfections, means that there can be a considerable uncertainty on the material parameters used in the computer simulations, even for relatively simple models such as the linear elastic orthotropic model. [6, 9, 10]

Considering the interaction between the material behaviour and the overall structural response, as well as the continuing work by CEN/TC 248 WG 5 towards a normative document regarding the design of tensile fabric structures, the ability to capture and understand these material-based variations is important. While some research exists applying a statistical approach to the tensile strength of fabric materials [11, 12], when it comes to interpreting the material's mechanical parameters existing studies are limited. Two main reasons for this are the lack of a standardised test methodology and the lack of a reasonably large data set which generates reliable statistical models.

In this paper, the consistency of the stress-strain results and derived material parameters obtained from the biaxial test profile proposed by the recently published EN 17117-1:2018 [13] has been investigated. Next, a methodology is outlined to describe the noted variability as stochastic distribution is proposed and evaluated against the data obtained from the biaxial tests assessing the method's possibilities and limitations.

In the next section, the test setup and methodology is explained as well as the process used to derive the material constants. Next, the immediate stress-strain results and derived material parameters are discussed, verifying consistency between the various tests. Finally, a methodology to statistically describe the linear elastic orthotropic material parameters and verify the goodness-of-fit of proposed stochastic distributions is explained and applied to the test data.

2. Test setup and derivation methodology

2.1. Biaxial test environment and samples

To generate the data discussed in this paper, a Type II polyester-PVC coated textile (Sioen T2103, [14]) was tested on the biaxial test bench available at the department of Mechanics of Materials and Constructions (MeMC) of the Vrije Universiteit Brussel. The biaxial test bench at the Vrije Universiteit Brussel consists of four hydraulic actuators mounted on a solid frame (figures 1 and 2, [6]). The actuators are translationally fixed to the frame and each actuator is equipped with a 100 kN-capacity load cell. These four load cells not only register the applied force for the respective actuator, but also allow the controller to balance the applied load to ensure a symmetric load application and as such avoid unwanted shear stresses as much as possible.

The cruciform samples used for these tests consist of a 30 cm by 30 cm central area with four slitted arms ending in a welded loop to connect to the biaxial test bench. Two additional cut-outs are required to accommodate the bar connection (figure 2, right). Their impact on the stress and strain fields was verified using preliminary measurements as well as an inter-laboratory comparison showing that these cut-outs did not impact the stress-strain results obtained from the center of the sample to a significant degree. [6]

The central area of the sample has been speckled with black paint, providing a randomised reference pattern for the three dimensional Digital Image Correlation (DIC) system utilised to determine the strain field. Two AVT Stingray F-504 cameras [15] were mounted 70 cm above the sample and were aligned so that the analysis directions follow the main fibre directions of the sample. These cameras take pictures of the sample at regular time intervals of 5 s and load intervals of 100 N, which ever one occurs first, allowing the extraction of material strains during the correlation process after the test. By routing the signal from the load cells through the DIC system, stress and strain measurements are synced, ensuring consistency in the results. The correlation of the DIC pictures was carried out using the commercial software package VIC 3D 2010 from Correlated

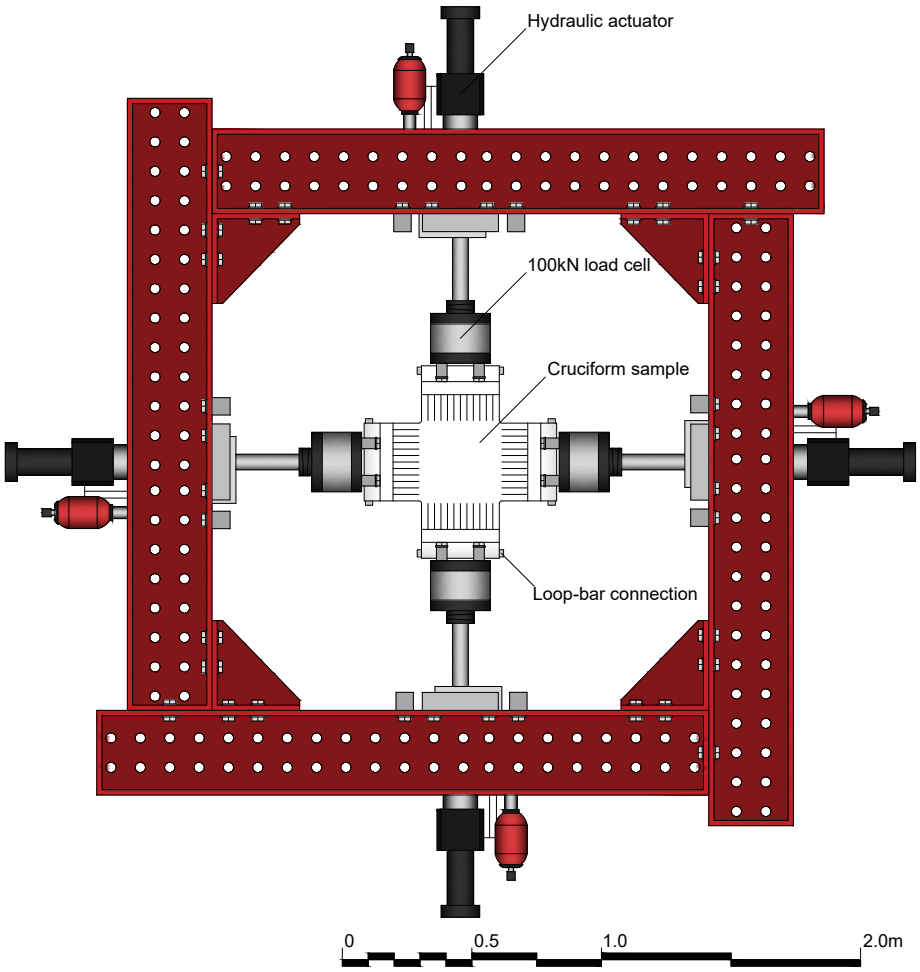

Figure 1: The biaxial test bench of the Vrije Universiteit Brussel consists of four hydraulic actuators translationally fixed on a steel frame. [6]

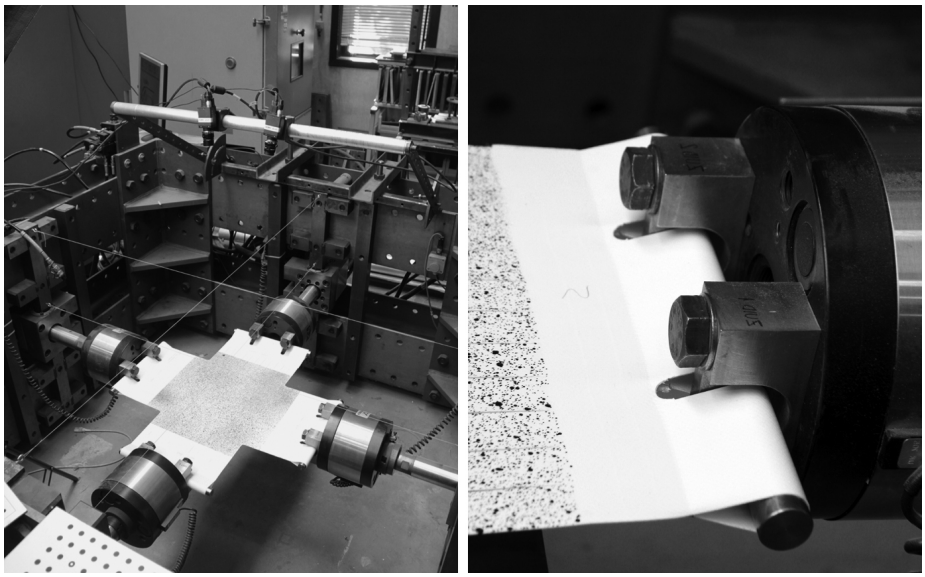

Figure 2: A sample with a central area of 30 cm by 30 cm can be fixed in the test bench (left). The used bar-loop system requires two cut-outs in each connection (right). [6]

Solutions [16]. To ensure consistency amongst the various tests, all results were correlated using the same settings presented in table 1.

As mentioned in the introduction, all ten tests were carried out utilising the load profile specified in EN 17117-1:2018 (Figure 3, top). This load profile cycles through four asymmetric load ratios, with a symmetric load ratio between each asymmetric ratio to normalise the fabric's strain state. EN 17117-1:2018 recommends an upper limit to the load of 25% UTS and a prestress level of 1% UTS. Due to limitations on the controller of the biaxial bench however, the lower load limit during the tests needed to be set at 2.5% UTS. With a manufacturer-specified tensile strength of 80 kN/m for the T2103 material [14], the theoretical stress at the centre of the sample should thus cycle between 2 kN/m and 20 kN/m. Taking into account the width of the sample (30 cm) the theoretical applied load thus cycles between 0.6 kN and 6 kN. These values do however not yet take into account the stress reduction effect present in biaxial samples [6, 17]. During preliminary research [6], the average stress reduction

Parameter	Value
Pre-filtering	Gaussian 5
Subset size	29 pixels
Step size	7 pixels
Correlation criterion	Zero-mean normalised sum of squared difference
Interpolation criterion	Optimised 8-tap spline
Strain filter size	9

Table 1: For consistency, all tests were correlated in Vic 3D 2010 using the same DIC correlation settings.

factor for the sample geometry used during this investigation has been established to be 95%. The theoretical applied force thus has to be increased to take this reduction into account, ensuring the appropriate stress is present in the center of the sample. Hence, the applied force becomes 0.632 kN at prestress level and 6.316 kN at maximum load, which are the effective values noted on the load profile shown on the bottom part of figure 3. From previous experience, a single load/unload cycle is set to take 342 s ensuring an appropriate overall displacement speed, resulting in an effective maximum load rate of 33 N/s during this load-controlled test for a total test duration of little over 2h15.

The registration of both the strains and applied loads us carried out by the DIC system. During these tests, the DIC system is set up to take pictures and register the load data of each individual actuator every 0.1 kN or every five seconds, whichever one occurs first. The outcome consists of around 2700 data points for both the applied forces (which are processed to material stresses) and strains, or an average of one picture every three seconds over the entire test duration.

2.1.1. Strain measurement area

As the DIC system can extract strains using various measurement tools (point-wise, according to a line, or averaged over a specific area), it should be

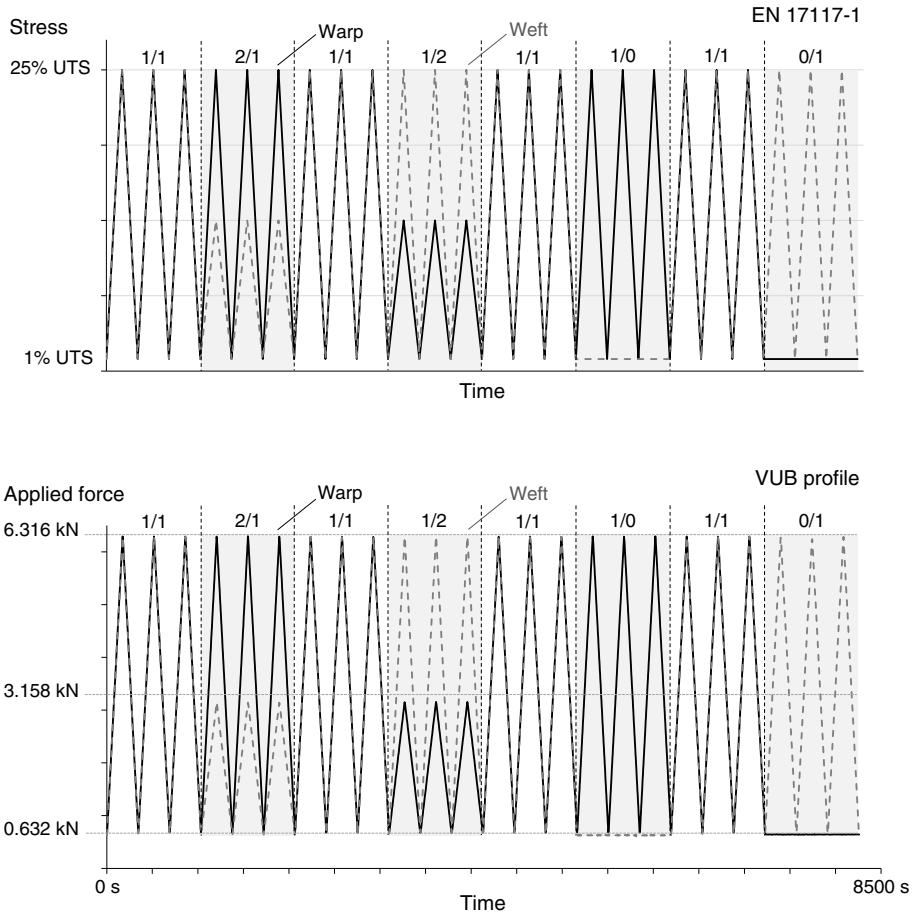

Figure 3: While EN 17117-1:2018 provides a suggested load profile (top, [13]), the prestress level had to be increased from 1% to 2.5% for the presented tests (bottom).

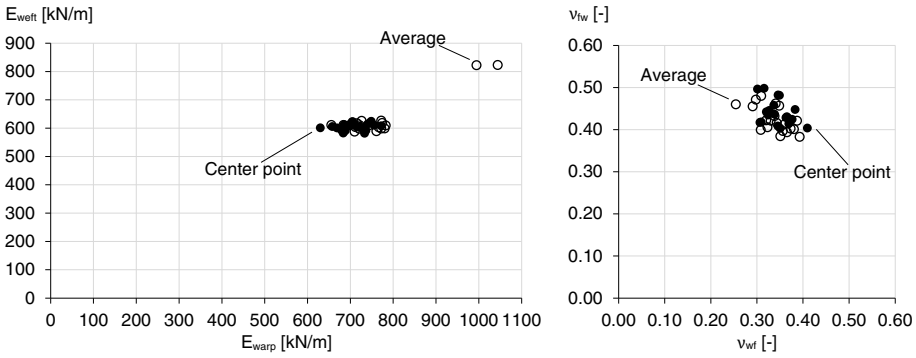

Figure 4: Averaging the DIC strain results over a 5 cm by 5 cm area around the sample's central point ("average") resulted in outliers compared to the consistent results obtained from strains extracted from the center point ("center point").

clearly specified which area-of-interest was used for the results obtained in the next sections. As EN 17117-1:2018 does not provide a clear guideline in this regard and simply specifies that "*strain measurement should be made within a field of homogeneous strain*" [13], different approaches could be considered.

Nonetheless, the requirement of a homogeneous strain field (variations $<$ 5% of the measured strain in both directions) does impose some restriction. As shown above, the mounting solution currently used on the biaxial bench requires that the sample's loop comes with a pair of cut-outs on each arm. Although previous experiments have shown that these cut-outs have a limited effect on the central area of the sample [6, 10], they do still affect the stress and strain uniformity of the larger area around the center point. This effect will become more important when asymmetries occur during the test due to e.g. control inaccuracies. Hence, during the processing of the test results, strains were extracted using 2 methods: (1) take the average result of a 5 cm by 5 cm square area around the sample's center point ("average"), and (2) extract the strains point-wise from the center of the sample ("center point"). While the first method is less susceptible to local outliers as compared to the second method, it can be affected by non-uniform strain fields potentially influencing the results of the test.

By comparing the derived material constants from both methods (figure 4), it turned out that the strains extracted from the central point yielded more consistent results where the outcomes utilising the average strains led to some notable outliers. Consequentially, all of the following data and results presented in this paper were extracted using the strains from the center point rather than the averaged area. Through a currently ongoing re-design of the clamps to remove the need for the aforementioned cut-outs, it will become possible in the future to consider a bigger strain-measurement area.

2.2. Material parameter derivation

The stress-strain data obtained from the biaxial tests should then be post-processed to fit material constants to this data. The material constants that would be fitted depend on the desired numerical material model. Following the EN 17117-1:2018 document, this research has been limited to the linear elastic orthotropic material model consisting of two Young's moduli and two Poisson's coefficients.

Applied to fabrics, assuming a plane stress state, the linear elastic orthotropic material model is formulated by equation 1. Within this equation we note two Young's moduli E_{warp} and E_{weft}, one for each main fibre direction, as well as two Poisson's coefficients ν_{wf} and ν_{fw}. Shear strains, while included in the consecutive equation below, are typically disregarded while studying a fabric's biaxial behaviour as its contribution is assumed small considering the idealised orthotropic stress state generated by the biaxial test equipment.

$$\begin{bmatrix} \epsilon_{warp} \\ \epsilon_{weft} \\ 2\epsilon_G \end{bmatrix} = \begin{bmatrix} \frac{1}{E_{warp}} & -\frac{\nu_{fw}}{E_{weft}} & 0 \\ -\frac{\nu_{wf}}{E_{warp}} & \frac{1}{E_{weft}} & 0 \\ 0 & 0 & \frac{1}{G} \end{bmatrix} \begin{bmatrix} \sigma_{warp} \\ \sigma_{weft} \\ \sigma_G \end{bmatrix} \tag{1}$$

Due to the symmetry requirement of the compliance matrix, we know that the four main parameters are not fully independent. Through rewriting the symmetry equation we find that the ratio of the Young's moduli E_{warp}/E_{weft} should be equal to the ratio of the respective Poisson's coefficients ν_{wf}/ν_{fw}.

This relation is referred to in literature as the "reciprocal relation". This relation imposes an additional constraint on the linear elastic material model but the observed behaviour of fabrics often seems to violate this equality. Due to the non-homogeneity of the material and the presence of imperfections such as non-orthogonal fibre alignment or a imperfect coating adhesion, experimental results often differ from predictions made using the reciprocal relation. [18]

To obtain the linear elastic material parameters, the stress-strain data from the biaxial tests has been processed as specified in annex E of EN 17117-1:2018, detailing the methodology to derive *comparative* elastic constants. This means all unloading cycles were removed from the test results, only the last of the three cycles for each asymmetric load ratio was considered, as well as the last of the three first cycles of the symmetric 1:1 load ratio (see section 3.2). In addition, permanent strains were removed by normalising the stress-strain results at the start of each individual load cycle.

As specified by the same annex, estimated material parameters have been fitted to the experimental data using the least-squares method. During the fitting process the reciprocal constraint has not been explicitly enforced and best-fit parameters were derived by either minimising the stress difference or the strain difference [13, 19]. The outcome consists of two sets of material parameters for each of the conducted tests, providing us with a total of 20 sets for further analysis and discussion in the next sections.

3. Interpreting biaxial test results

Before proceeding to the statistical analysis, the direct results from the biaxial tests were evaluated to better comprehend the consistency/variability we can expect from running multiple tests using the load profile proposed by EN 17117-1:2018. During this evaluation, direct strain measurements were compared as well as the stress-strain curves of the various load ratios. The goal of this interpretation of raw test data is to verify the immediate consistency of the 10 tests that were carried out as it will provide a first estimate of what we

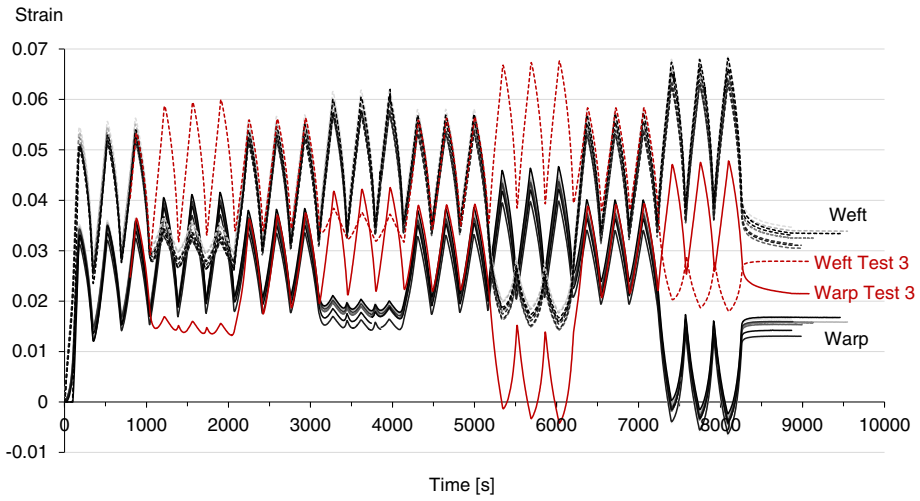

Figure 5: All tests showed comparable time-strain results, with the exception of Test 3 where the sample was wrongly oriented within the test bench.

can expect of the material properties and their statistical properties. After the comparison of the raw test data, the linear elastic material constants were derived and shortly discussed.

3.1. Time-strain results

Observing the direct strain output obtained from the DIC system in function of the time, which is recorded simultaneously with the DIC pictures, the majority of the measurements look consistent. The outcome of one test however, namely test 3, deviates from the bulk of results (figure 5). This is due to a misalignment of the sample before the tests, effectively switching the warp en weft direction of the sample. Consequentially, the test's asymmetric load ratios for this test are switched around which can be clearly noted on the graph. To what extent this affects the derived material constants will be evaluated in the next section, but previous studies have already indicated that switching around only the asymmetric load ratios does not impact the derived material constants to a significant degree when the test profile contains intermittent 1:1 load ratios to normalise the fabric [20].

Important to note here is that differences in the time-strain graphs do not necessarily lead to a difference in the derived material constants. Since the presented strains are measured by the DIC system by comparing the stressed state to a chosen reference state, slight changes in the reference state tend to cause notable differences in the presented strains. During the derivation of the material parameters however, strains are normalised by observing the strains relative to the start of the relevant loading cycle. In the graph above, this corresponds to the relative height of the peaks rather than the absolute location of the strain graph. To better compare the obtained measurements, stress-strain graphs provide a much clearer insight in how the conducted tests compare to each other.

3.2. Stress-strain data

When it comes to estimating how the different material constants derived from the various tests relate, stress-strain diagrams provide more comprehensive information than the time-strain data. For the graphs presented below, the load cycles that were used during the parameter derivation were extracted (figures 6), the unloading curve was removed, and stresses and strains were normalised at the prestress level. The result is a set of stress-strain curves showing the variation on the experimentally measured stress-strain behaviour between the different tests (figure 7).

These normalised stress-strain curves show that all ten tests provide relatively consistent results, with only minor variations which are not uncommon for a coated textile's biaxial behaviour. As a consequence, we can expect the derived material constants to reflect a similar consistency although some variation between the different test results will likely still exist.

4. Derived material parameters

While the established stress-strain relations already show how the various tests relate to each other in terms of consistency, these results are typically

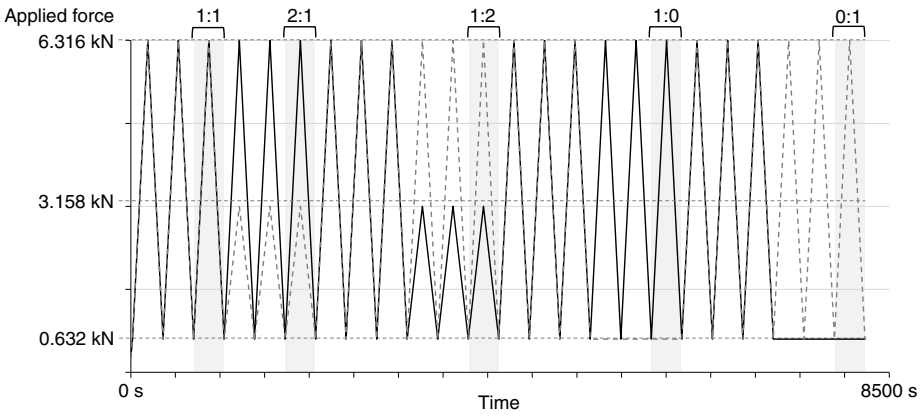

Figure 6: For the derivation of the material constants, five load ratios were selected.

further processed for use in Finite Element Models to model the behaviour of tensile fabric structures. While the exact methodology differs in function of the type of material model used for these simulations, the methodology used for this particular research comes from EN 17117-1:2018.

As mentioned before, the derived material constants, namely two Young's moduli and two Poisson's coefficients, describe a linear elastic orthotropic material model. As specified in annex E of EN 17117-1:2018 the derived constants only use the loading part of the five selected load cycles, with each curve being normalised before deriving the constants, utilising the least squares method to fit the model's parameters to the experimental results. During the data processing, the measured forces are divided by the sample's width (0.3 m) and multiplied with the stress reduction factor (0.95) to convert forces applied at the ends of the sample to membrane stresses in the center of the sample. All data processing has been carried out in MATLAB R2015a [21] utilising the built-in *patternsearch()* function to carry out the least square minimisation.

Note that, as specified in EN 17117-1:2018, the reciprocal relation has not been enforced which means that the derived material constants will likely not adhere to the reciprocal relation. While this means that the derived constants are not directly applicable in the linear elastic material model, the statistical analysis

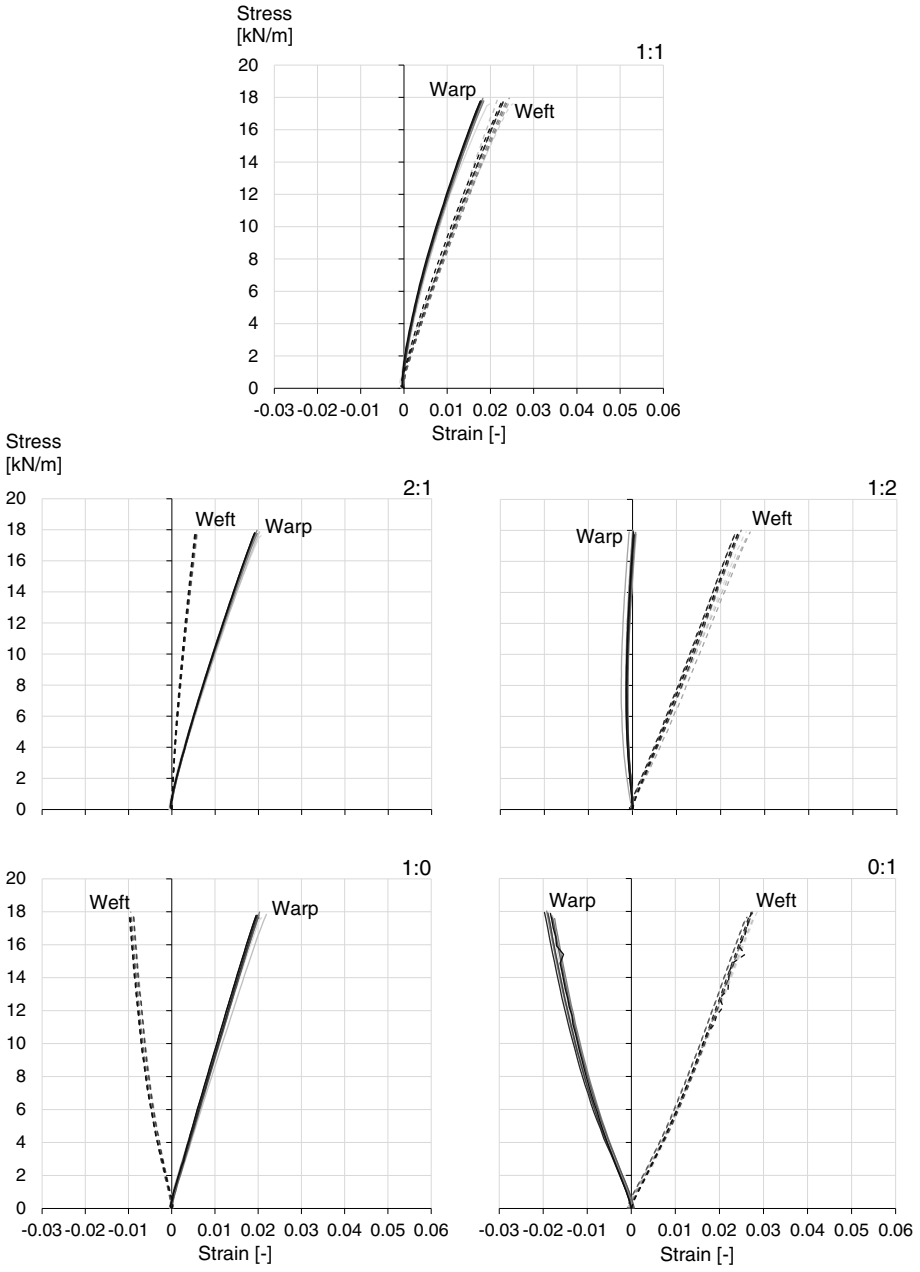

Figure 7: The normalised stress-strain curves of each relevant load ratio of all ten tests show a reasonable consistency between the different tests. For increased readability, the dominant stress direction was used to represent both fibre direction graphs.

we will be describing and carrying out in the next section would inherently break the reciprocal relation as well. Considering that fabrics do not adhere to this relation [18, 22], the specifications laid out in EN 17117-1:2018, and the effect further analysis has on the material constants, it makes sense to disregard the reciprocal relation from the described material parameter derivation and further analysis at this stage of the research.

4.1. Discussing the derived material parameters

Running the derivation process for all ten biaxial tests, using both stress and strain minimisation methods, leads to the 20 sets of material constants presented in table 2.

Drawing these sets on two graphs, one containing both Young's moduli (figure 8, left) and one containing both Poisson's coefficients (figure 8, right), clearly shows the variability of the results. When it comes to the Young's moduli, E_{warp} shows a relatively large variation of around 150 kN/m while the variation on E_{weft} is relatively small spanning below 50 kN/m. By comparison, the variation on both Poisson's coefficients is fairly similar with both ν_{wf} and ν_{fw} showing a variation of around 0.1, with the average value of ν_{fw} lying slightly higher than the average of ν_{wf}. This latter is typical for sets of material parameters derived without enforcing the reciprocal relation [6, 10].

These results show that even when a singular material of the same batch is tested on the same setup utilising the same load profile for all tests, a certain level of variation can still be expected due to the complex nature of coated woven textiles. Small variations such as the relative orientation of the main fibre directions, minor defects in the sample and/or coating, etc. affect the outcome of each test leading to a variation on the derived material parameters. While the exact magnitude of this variation will depend on the textile that was tested, and the fitted material model, a certain degree of variation is inherent to the nonlinear anisotropic textile material.

		E_{warp} $[kN/m]$	E_{weft} $[kN/m]$	ν_{wf} $[-]$	ν_{fw} $[-]$
Test 1	stress min.	688.23	590.79	0.3382	0.4366
	strain min.	736.36	591.75	0.4326	0.3784
Test 2	stress min.	679.74	592.51	0.3090	0.4181
	strain min.	731.22	592.42	0.3501	0.4034
Test 3	stress min.	629.92	601.06	0.3155	0.4982
	strain min.	668.73	600.56	0.3457	0.4822
Test 4	stress min.	683.45	582.68	0.3203	0.4423
	strain min.	733.27	581.90	0.3650	0.4306
Test 5	stress min.	704.02	622.58	0.3064	0.4171
	strain min.	747.91	622.67	0.3452	0.4086
Test 6	stress min.	657.88	605.54	0.3010	0.4963
	strain min.	714.29	605.41	0.3488	0.4815
Test 7	stress min.	705.88	622.59	0.3240	0.4347
	strain min.	748.98	624.15	0.3629	0.4286
Test 8	stress min.	698.08	610.08	0.3265	0.4454
	strain min.	755.46	610.35	0.3674	0.4272
Test 9	stress min.	685.45	612.51	0.3365	0.4579
	strain min.	740.52	614.64	0.3828	0.4478
Test 10	stress min.	722.05	606.51	0.3691	0.4141
	strain min.	772.15	608.22	0.4094	0.4037

Table 2: Overview of the derived sets of material parameters from the 10 conducted biaxial tests.

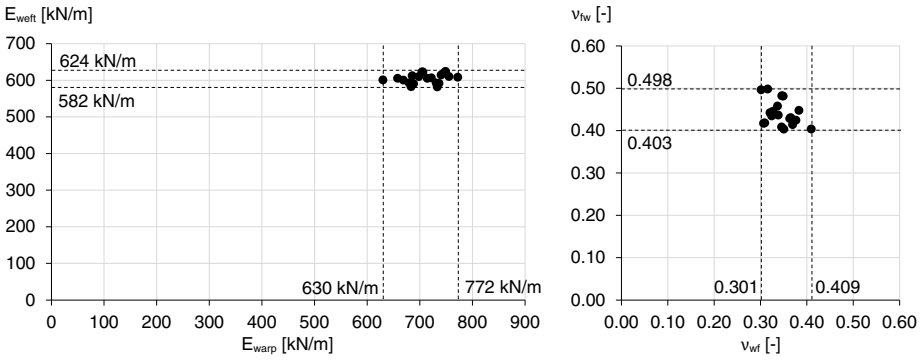

Figure 8: The resulting 20 sets of material parameters do show a relatively large variation of almost 150 kN/m for E_{warp}, but are otherwise reasonably consistent for each of the 4 parameters.

5. Statistical interpretation of material constants

With CEN/TC 248 working on the standardisation of the use of coated textiles in engineering, being able to describe the variability and uncertainty that exists on derived material parameters is important to assess structural safety and carry out reliability analyses on tensile fabric structures [11, 23]. In this section, a general approach is laid out to describe the derived material constants statistically, ensuring the established distributions are indeed compatible with the derived material constants. While this seems relatively straightforward, the main challenge in this regard is the fact that typical statistical normality tests such as the Kolmogorov-Smirnov (KS) and the Anderson-Darling (AD) test assume an independence between the data and the proposed distribution [24]. However, since we will derive a distribution from the data using the Maximum Likelihood Estimate (MLE) method, the approach below requires some additional steps to remove statistical bias due to the resulting dependency between the data and the proposed distribution. Applying this methodology on the data described above will then not only provide an idea of the statistical properties of the results obtained from the conducted tests, but also illustrate the possibilities as well as limitations of the utilised approach.

5.1. Method to establish and verify distributions

The first step of the analysis method consists of deriving the Maximum Likelihood Estimate (MLE) for each of the four material parameters and deriving the Cumulative Density Function (CDF) of the resulting distribution. In general, the MLE is defined as follows:

$$\hat{\theta}_{MLE} = \underset{\theta \in \Omega}{max} f(x|\theta) \tag{2}$$

The equation above estimates the value for the vector θ, within a parameter space Ω, so that the probability of the observed dataset x being generated by the proposed probability distribution is maximised. During this study Matlab's *mle()* function was utilised to estimate the respective distribution parameters for each distribution family from the obtained material constants.

As mentioned before, doing this means that the derived distribution is not independent from the studied data set which is one of the main requirements to verify the goodness of fit using the KS or AD test. Both of these tests rely on so called test statistics which are compared to tabulated values to verify whether or not we can reject the null hypothesis that the distribution is compatible with the data. For both the KS and AD test when the test statistic, respectively $\bar{D}_n$ and $\bar{A}_n^2$, is smaller than the appropriate tabulated value the null hypothesis can not be rejected, making it plausible that the proposed distribution is indeed compatible with the data. The test statistics $\bar{D}_n$ and $\bar{A}_n^2$ are derived as follows:

$$\bar{D}_n = \underset{1 \leq i \leq n}{max} |F(x_i) - \frac{i-1}{n}, \frac{i}{n} - F(x_i)| \tag{3}$$

$$\bar{A}_n^2 = -n - \frac{1}{n} \sum_{i=1}^{n} (2i-1)[ln(F(x_i)) + ln(1 - F(x_{n+1-i}))] \tag{4}$$

where F is the proposed cumulative density distribution, and n the length of the data set. Note that, the data x_i should be ordered from low to high for these tests to work properly. The equations above show a clear difference in the approach each test takes. Where the Kolmogorov-Smirnov test evaluates the largest vertical difference (i.e. the largest difference in cumulative probability

for a specific data value), the Anderson-Darling takes a more weighted approach by considering the sum of the difference in natural logarithms. Despite their differences, both tests assume independence between the proposed distribution and the tested data set [24] which, as mentioned above, is not the case when using the MLE method.

A possible solution to counteract this data-distribution bias is to generate B ($\in \mathbb{N}$) re-sampled bootstrap sets from the derived distribution function, each the same size as the original dataset (n) [25]. The generated samples B are, by definition, compatible with the proposed distribution. Knowing this, we can derive the MLE as well as the corresponding KS and AD test statistics. These new values allow us to estimate the variability that is to be expected on the MLE distributions and test statistics when the data and proposed distribution are compatible. We can thus set a level of significance α and select the $1-\alpha$ quantile of the found test statistics, respectively $\bar{D}^*_{1-\alpha}$ and $\bar{A}^{2*}_{1-\alpha}$. These values will then serve as new critical values instead of the tabulated values to verify whether or not we can reject the null hypothesis. Hence during the upcoming analysis we will consider the derived distribution compatible under the KS and AD test respectively when:

$$\begin{gathered} \bar{D}_n < \bar{D}^*_{1-\alpha} \\ or \\ \bar{A}^2_n < \bar{A}^{2*}_{1-\alpha} \end{gathered} \tag{5}$$

For the analysis described in this paper, the significance level α was set to 0.05 and a total of 1000 bootstrap samples were generated to obtain a good estimate for the critical values. The bootstrap samples were generated utilising Matlab's *bootstrap()* function, utilising three distribution families: normal, lognormal and Generalised Extreme Value (GEV). This latter is a generalised function containing three subcategories, namely, the Gumbel, Fréchet, and Weibull distributions (respectively a "type I", "type II", and "type III" GEV distribution).

5.2. Step-wise data processing

The methodology utilised during this research thus comes down to various steps, starting from the processed test data up to the evaluation of the proposed statistical distributions to describe the properties of the obtained material constants.

1. Derive the Maximum Likelihood Estimate parameters for each of the three distribution families, for each of the four material constants.
2. Calculate the respective test statistic for each parameter-distribution combination under both the Kolmogorov-Smirnov and Anderson-Darling test.
3. Account for bias by re-sampling B sets from the estimated distribution by bootstrapping, derive the MLE for each of the samples and derive their test statistics.
4. Calculate the $1 - \alpha$ quantile value for each respective test statistic, setting α to the desired level of significance (in this case $\alpha = 0.05$).
5. Use the resulting values as the new respective critical values to assess compatibility with the respective distribution and material parameter at the significance level α. Compare the derived statistics from step 1 to the new critical values and reject the distribution if the derived value exceeds the critical value.

The result of this approach consists of a compatibility assessment for three distribution families for each of the four individual material constants. As a consequence, any potential correlation between the four material parameters is removed from the equation. While this is not directly relevant to the scope of this paper, it should be kept in mind when e.g. deriving least-advantageous parameters from the statistical distributions as one might end up with a non-representative set of material parameters [6].

5.3. Application to the test data

By applying the described procedure to the derived linear elastic orthotropic non-reciprocal material parameters, the potential as well as the limitations

	Normal		Lognormal	
	μ	σ	μ_{log}	σ_{log}
E_{warp}	710.1798	35.6311	6.5642	0.0507
E_{weft}	604.9467	12.7932	6.4049	0.0212
ν_{wf}	0.3450	0.0278	-1.0674	0.0801
ν_{fw}	0.4399	0.0287	-0.8232	0.0639
	Generalised Extreme Value			
	shape k	*scale* σ_{GEV}	*location* μ_{GEV}	
E_{warp}	-0.4645	38.1434	700.8004	
E_{weft}	-0.5868	14.4158	602.3928	
ν_{wf}	-0.1604	0.0254	0.3337	
ν_{fw}	0.1334	0.0204	0.4253	

Table 3: Overview of the MLE parameters for each material constant and distribution family.

of the aforementioned methodology can be assessed. In this part each step of the process is documented. Further discussion regarding the outcome and observations made during this analyses can then be found in the next part.

5.3.1. Deriving the MLE parameters

Applying Matlab's *mle()* function to each of the four sets of material constants provides us with three candidate distributions for each material constant. The respective distribution parameters are listed in Table 3.

While compatibility of the derived distributions is yet to be verified, the values presented in table 3 do give some insight in the underlying data. For one, the notable difference in variation between E_{warp} and E_{weft} appears clearly in the standard deviations of both the normal and lognormal distributions, σ and σ_{log} respectively. Looking at the results of the GEV distributions, all proposed distributions except the one for ν_{fw} correspond to a Type III, or Weibull, distribution since the shape factor $k < 0$. The proposed distribution for ν_{fw} on the other hand corresponds to a Type II, or Fréchet, distribution since

	Normal		Lognormal		GEV	
	$\bar{D}_n$	$\bar{A}_n^2$	$\bar{D}_n$	$\bar{A}_n^2$	$\bar{D}_n$	$\bar{A}_n^2$
E_{warp}	0.1226	0.2021	0.1261	0.2233	0.0931	0.1526
E_{weft}	0.1345	0.3749	0.1339	0.3806	0.1485	0.5423
ν_{wf}	0.0971	0.2010	0.0945	0.1902	0.1053	0.1961
ν_{fw}	0.1466	0.7047	0.1349	0.6017	0.1089	0.2131

Table 4: The (biased) test statistics of each distribution family for each of the four material constants.

$k > 0$.

5.3.2. Calculating the biased test statistics

With the derived distributions established, their compatibility with the data should be verified. As mentioned before, both the Kolmogorov-Smirnov and Anderson-Darling tests will be used. For each parameter and derived distribution, both Kolmogorov-Smirnov (KS) and Anderson-Darling (AD) test statistics were derived (Table 4).

Typically, when the proposed distribution is not derived from the related dataset, the critical values for these test statistics are listed in function of the size of the data set and the significance level in published tables [24, 26]. For this data set of 20 elements at a significance level of 0.05, the critical KS statistic $\bar{D}_{crit} = 0.2941$ and the critical AD statistic $\bar{A}^2_{crit} = 2.5019$. However, due to the dependence of the proposed distributions on the underlying data set, these standard critical values are inappropriately large for this case. As a result, all the derived test statistics fall below these two critical values. In the next step, we will generate bootstrapped samples which will allow us to derive appropriate critical values at the chosen level of significance for both the KS and AD test statistics.

	Normal		Lognormal		GEV	
	$\bar{D}_{0.95}$	$\bar{A}^2_{0.95}$	$\bar{D}_{0.95}$	$\bar{A}^2_{0.95}$	$\bar{D}_{0.95}$	$\bar{A}^2_{0.95}$
E_{warp}	0.1916	0.7228	0.1916	0.7284	0.1850	1.8425
E_{weft}	0.1934	0.7550	0.1969	0.7625	0.1933	2.1348
ν_{wf}	0.1954	0.7547	0.1913	0.7080	0.1706	0.5978
ν_{fw}	0.1883	0.7150	0.1885	0.7067	0.1714	0.5617

Table 5: Test statistics of each distribution family for each material constant after the bootstrapping process which removes bias.

5.3.3. Determine the bootstrapped test statistics

To determine the effective critical values for the test statistics for the biased case, the data is bootstrapped/re-sampled using the estimated distribution. For each re-sampled set, a maximum likelihood estimate distribution is derived after which the test statistics are calculated. The end result is a set of test statistics from which we can select the n-th percentile value at a chosen level of significance. As mentioned before, for the research presented in this paper we set the level of significance at 0.05. As such we accept a 5% chance that a compatible distribution is rejected. Note that the higher we set the level of significance (e.g. 0.1 or 0.15), the more restrictive our critical value becomes and more compatible solutions will end up being rejected (respectively 10% and 15%).

Utilising 1000 bootstrapped samples, the resulting quantiles $\bar{D}_{0.95}$ and $\bar{A}^2_{0.95}$ of the test statistics for each material parameter and distribution type are presented in table 5.

As expected, these new critical values are significantly lower than the tabulated values for $\bar{D}_{crit}$ and $\bar{A}^2_{crit}$, 0.2941 and 2.5019 respectively, illustrating how this methodology takes into account the bias due to data-distribution dependency by reducing the critical test statistic values accordingly.

	Normal		Lognormal		GEV	
	P_{KS}	P_{AD}	P_{KS}	P_{AD}	P_{KS}	P_{AD}
E_{warp}	0.5800	0.8810	0.5670	0.8370	**0.8990**	**0.9700**
E_{weft}	0.4330	**0.4120**	**0.4660**	0.4100	0.2640	0.2520
ν_{wf}	**0.8970**	0.8850	0.8650	**0.9240**	0.7050	0.8000
ν_{fw}	0.2890	0.0540	0.4640	0.1140	**0.6350**	**0.7390**

Table 6: Interpreting the test outcomes as P-values, a quantitative comparison can be conducted, looking for the highest P-value for each test and parameter (bold).

5.3.4. Compare the initial values to the newly-established critical values

Comparing the test statistics presented in table 4 to the derived critical values presented in table 5 allows us to evaluate the effective compatibility between the established maximum likelihood estimated distributions for each of the four material parameters and the data from the biaxial tests. Doing so, we should bear in mind that we are not proving compatibility through this method, but rather can not rule out compatibility when the test statistic is smaller than the critical value.

When we do this for the obtained results, it turns out we can not rule out any of the proposed distribution based on either the KS and AD test statistics. Listing the corresponding P-values for each test (table 6), allows us to compare the different distributions qualitatively. Higher P-values indicate a closer correspondence between the proposed distribution and the underlying data. Note that this latter isn't a typical interpretation, and P-value analysis of these tests usually limit themselves to rejecting or not rejecting the distribution based on whether or not the value lies below the chosen level of significance. With all proposed distributions compatible however, it does allow us to assess the relative distance between the data and the proposed distribution.

Observing the P-values shows that although we couldn't rule out any of the proposed distributions, there are some differences visible: for E_{warp} and ν_{fw} the higher P-value is obtained for the GEV distribution, and the outcomes for

E_{weft} and ν_{wf} show the values for the normal and lognormal distribution close to each other and exceeding the outcome for the GEV distribution. The results above however indicate that capturing all four individual parameters through one distribution family might not be feasible.

Utilising the methodology described above, it thus becomes possible to characterise the four linear elastic orthotropic material constants using a statistical description rather than simple test averages. This allows us to e.g. use their intrinsic variability in reliability analyses or try and compose a set of least-favourable parameters. When doing this latter, which lies outside the scope of this paper, attention should be paid to ensure the obtained set respect possible correlations that exist between the different material parameters.

5.4. Remarks and discussion

The methodology outlined above illustrates how a fabric's material parameters can be described by statistical distributions. These distributions can be useful from various points of view, being for manufacturers specifying ranges for their materials, to implementing the material's mechanical behaviour as an uncertain parameter in reliability analysis.

The presented research is however still somewhat limited on various of points. In this section a reflection is made on some of these limitations, such as the limited amount of data points and the convergence of the bootstrapped results, as well as the impact of the removal of the reciprocal constraint during the derivation of the material parameters.

5.4.1. The effect of the reciprocal relation

As mentioned before, the analysis above was conducted without applying the reciprocal relation between the ratio of the Young's moduli and Poisson's ratios according to the recommendations presented in EN 17117-1:2018. Removing this restriction however leads to physical meaningless sets of material constants and shifts certain values. But what does applying this restriction mean for the analysis presented above?

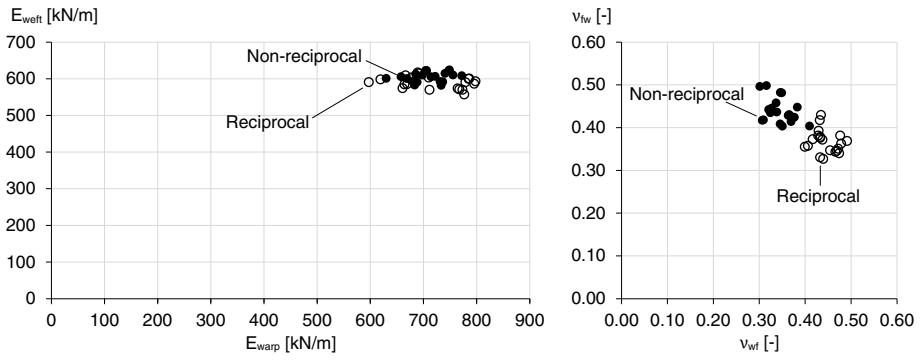

Figure 9: When enforcing the reciprocal constraint during material parameter derivation, the values of ν_{wf} become notably higher while the values for ν_{fw} decrease as compared to the non-reciprocal values.

Comparing the general scatter plots of the material parameters with and without the reciprocal relation applied, immediately shows the difference between these two data sets (figure 9). In terms of E_{warp}, the variation increases slightly with a distinct gap around 740 kN/m. This gap presents a notable discontinuity in the data leading to both an increase in the standard deviation and an increased difficulty to describe the data using a continuous function. While the Poisson's ratios do not show such discontinuities, the values of both ν_{wf} and ν_{fw} do decrease significantly when applying the reciprocal constraint to the data.

Running the same statistical analysis on the reciprocal material constants, leads to the MLE distributions detailed in table 7.

Comparing the biased KS and AD test statistics (table 8, top) to the bootstrapped critical values (table 8, bottom), clearly illustrates the difference between this data set and the previous one. Where none of the tests failed before, all but the GEV distribution end up being rejected for E_{warp}, as we expected. The GEV distributions that can't be rejected only differ from the critical value by a small margin, making it likely to be rejected at higher levels of significance.

Applying the reciprocal constraint thus not only forces the derived sets to adhere to behaviour that is not observed in practice for this material, but also possibly introduces data gaps making the fitting of statistical distributions

	Normal		Lognormal	
	μ	σ	μ_{log}	σ_{log}
E_{warp}	719.0521	61.3360	6.5742	0.0868
E_{weft}	589.6416	16.0676	6.3791	0.0273
ν_{wf}	0.4451	0.0252	-0.8111	0.0565
ν_{fw}	0.3665	0.0259	-1.0061	0.0693
	Generalised Extreme Value			
	shape k	*scale* σ_{GEV}	*location* μ_{GEV}	
E_{warp}	-1.0343	80.4339	720.2372	
E_{weft}	-0.4388	16.9990	585.2082	
ν_{wf}	-0.3200	0.0250	0.4367	
ν_{fw}	-0.0421	0.0213	0.3550	

Table 7: Overview of the MLE parameters for each material constant and distribution family utilising reciprocal sets of material parameters.

	Normal		Lognormal		GEV	
	$\bar{D}_n$	$\bar{A}^2_n$	$\bar{D}_n$	$\bar{A}^2_n$	$\bar{D}_n$	$\bar{A}^2_n$
E_{warp}	0.2195	0.8396	0.2221	0.8211	0.2204	2.3422
E_{weft}	0.1309	0.2803	0.1300	0.2905	0.1286	0.2501
ν_{wf}	0.1920	0.6758	0.1816	0.6467	0.1938	0.6791
ν_{fw}	0.1310	0.3423	0.1194	0.2666	0.0944	0.1724
	$\bar{D}_{0.95}$	$\bar{A}^2_{0.95}$	$\bar{D}_{0.95}$	$\bar{A}^2_{0.95}$	$\bar{D}_{0.95}$	$\bar{A}^2_{0.95}$
E_{warp}	0.1900	0.7282	0.1924	0.7156	0.2343	2.7923
E_{weft}	0.1893	0.7149	0.1955	0.7573	0.1790	1.9580
ν_{wf}	0.1933	0.7733	0.1953	0.7093	0.1751	0.7212
ν_{fw}	0.1940	0.7563	0.1880	0.7076	0.1702	0.5614

Table 8: Overview of the biased (top) and unbiased (bottom) test statistics for the reciprocal sets of material parameters.

difficult, if not impossible.

5.4.2. Convergence study

The accuracy of the conclusions made in the previous parts strongly depends on the reliability of the derived critical test statistics and distributions. As part of the bootstrapping routine involves sampling random data, the effective outcome (in our case $\bar{D}_{0.95}$ and $\bar{A}^2_{0.95}$) of the process is always slightly different. Hence, we need to ensure the amount of bootstrap samples we use is sufficient to avoid unintentionally skewing the outcome.

A convergence study was thus carried out, simulating 100 runs of bootstrapping for different amounts of samples, ranging from 10 samples up to 1500 samples. For each set of 100 bootstrap runs, the statistical properties of the resulting 0.95 test statistics for each of the three distributions was verified for E_{warp}. Ideally, the mean of these values should converge towards a specific value while the standard deviation σ becomes as small as possible to reduce the variance between different bootstrap runs.

Observing the effect of increasing the amount of bootstrapped samples on the test statistics $\bar{D}_{0.95}$ and $\bar{A}^2_{0.95}$, and the standard deviation σ, clearly shows convergence (figure 10). While for the KS test statistic $\bar{D}_{0.95}$ the mean value remains relatively constant while the standard deviations decreases quickly (figure 10, left), the AD test statistic $\bar{A}^2_{0.95}$ takes longer to converge (figure 10, right). In both cases however, the 1000 bootstrapped samples used in the previous parts showed to be sufficient to reach accurate results. An increase to 1500 samples could slightly increase the accuracy of the results, but it would only have a limited effect while increasing calculation time notably.

5.4.3. Influence of the sample size

Aside from the amount of bootstrap samples, the size of the actual data set will also be important. The investigation described above utilises data obtained from ten biaxial tests. Through deriving material parameters using both stress and strain minimisation leads to a set containing 20 data points. As the reliability

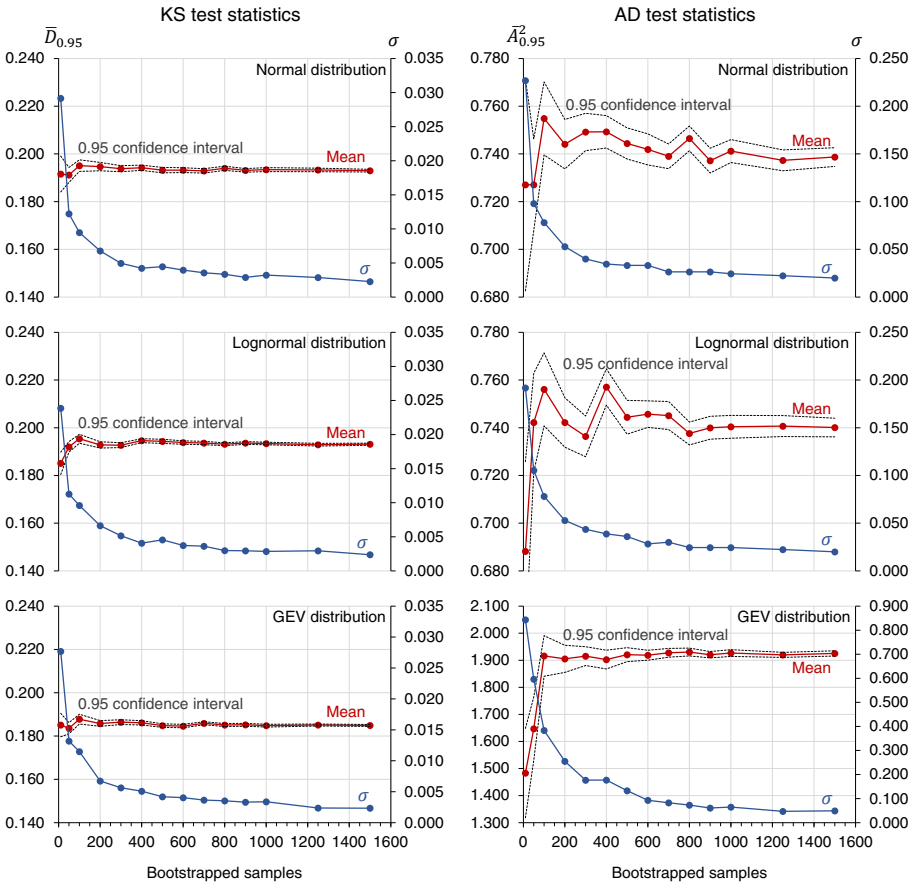

Figure 10: Observing the standard deviation and 0.95 confidence interval for the amount of bootstrap samples shows than 1000 samples was sufficient to obtain an accurate result.

of the fitted statistical models depends greatly on the sample size, some attention should be spend to this.

The main challenge with limited datasets is the potential of bias and inaccurate estimations of the underlying distribution. In our specific case, this might mean that the established variability and standard deviation are potentially smaller than they should be to properly describe the material's statistical properties. However, this bias can be removed by increasing the amount of conducted tests, possibly expanding to an international study where additional parameters such as different test conditions can be taken into account when describing the resulting parameters' variability.

Another effect of relying on a small dataset, is a relatively large variability in bootstrapped statistics. As each bootstrapped sample has the same size as the original data sample, the distributions derived from each of the 1000 re-sampled datasets tend to show a relatively large variation (figure 11, left). Increasing the size of the initial dataset would allow for an increase in the size of the sampled data during bootstrapping which would not only lead to a more accurate estimation of the initial distribution, but also reduce the variation of the bootstrapped distribution, effectively increasing the accuracy of the derived test statistics. This effect was artificially simulated by increasing the bootstrapped data points in figure 11 (right), but in reality this would also require the amount of effective data points (i.e. test results) to increase.

Given the only recent emergence of a standard regarding carrying out biaxial tests on coated textiles and deriving linear elastic orthotropic material parameters, there are very limited sources we can draw on the expand our data set at this point. Nonetheless, as statistical data representation is of primordial importance in normative documents, and a strong interaction between a fabric's mechanical properties and the overall structural behaviour exists, an international standardised benchmark generating the required data would be extremely useful to produce further insights into how we can integrate material parameters in statistics-dependent reliability analysis.

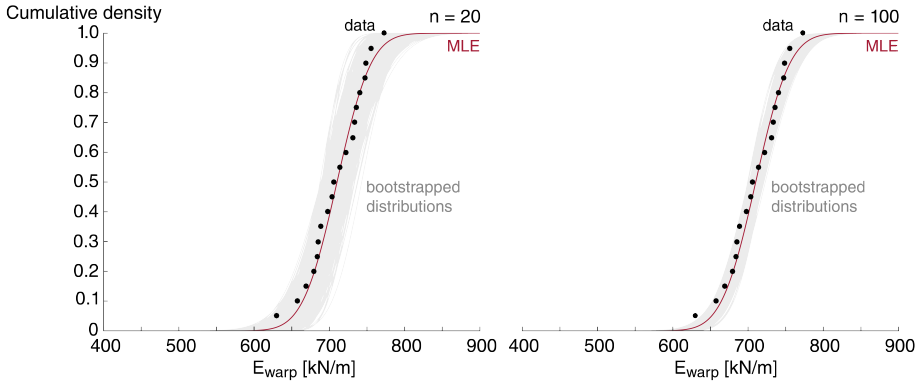

Figure 11: Increasing the sample count of the underlying data set from 20 (left) to 100 (right) would greatly reduce the variability on the bootstrapped distributions and thus increase the accuracy of the conducted normality tests.

6. Conclusions

This paper describes the test results obtained from ten biaxial tests on a Type II polyester-PVC fabric and conducted according the suggestions provided in the recently published EN 17117-1:2018 document. Linear elastic orthotropic material constants were derived and compared after which a stochastic analysis methodology has been laid out. This latter allows to describe each of the four material constants using its stochastic properties, taking into account the variability/uncertainty on each individual parameter.

The stress-strain curves obtained from the tests show only limited differences between each of the ten conducted tests. Similarly, the derived material constants are comparable. The biggest variation turned out to exist for the warp stiffness E_{warp} equalling to 150 kN/m.

To describe the stochastic properties of each parameter, a process known as bootstrapping has to be employed as for typical lab conditions the proposed distributions will usually be derived from the initial dataset using the Maximum Likelihood Estimates, thus introducing bias in the proposed distributions. Generating 1000 bootstrapped samples, and testing their compatibility using both the Kolmogorov-Smirnov and Anderson-Darling tests, allowed us to construct

compatible statistical distributions for each of the four material constants.

While the limited data set comprising only 20 sets of material parameters (two for each test) suggested all proposed distributions are compatible, artificially increasing the data size showed a clear decrease in uncertainty boundaries. Hence, the authors strongly encourage to carry out more tests according to the method published in EN 17117-1:2018 to increase the amount of data available as well as the accuracy of the derived stochastic distributions.

The methodology described in this paper thus allows to generate the basis required to incorporate the uncertainty on the material constants in e.g. reliability analysis, not only for fabric materials but various materials presenting a relatively large variability on test results. Alternatively, it could allow manufacturers to report more elaborate information regarding their materials while including the natural uncertainty that exists due to intrinsic material variations due to e.g. the manufacturing process.

Acknowledgements

The research presented in this paper was funded by the Research Foundation - Flanders (FWO) and was carried out the department of Architectural Engineering of the Vrije Universiteit Brussel. The biaxial tests presented in this paper were carried out in the scope of a master's thesis and the authors would like to thank ir. arch. Valérie Declerc for her enthusiasm and rigorousness during this research.

Data availability statement

The raw/processed data required to reproduce these findings cannot be shared at this time due to technical or time limitations.

References

[1] B. Forster, M. Mollaert (Eds.), European Design Guide for Tensile Surface Structures, Brussels, 2004.

[2] N. Stranghöner, J. Uhlemann, F. Bilginoglu, K.-U. Bletzinger, H. Bögner-Balz, E. Corne, N. Gibson, P. Gosling, R. Houtman, J. Llorens, Others, Prospect for European Guidance for the Structural Design of Tensile Membrane Structures, 2016. doi:10.2788/967746.

[3] M. Motevalli, J. Uhlemann, N. Stranghöner, D. Balzani, Geometrically nonlinear simulation of textile membrane structures based on orthotropic hyperelastic energy functions, Composite Structures (223) (2019). doi:10.1016/j.compstruct.2019.110908.

[4] G. Colasante, P. Gosling, Including shear in a neural network constitutive model for architectural textiles, in: TENSINET – COST TU1303 International Symposium 2016: Novel structural skins - Improving sustainability and efficiency through new structural textile materials and designs, Elsevier, Newcastle upon Tyne, 2016.

[5] A. Colman, B. Bridgens, P. Gosling, G. Jou, X. Hgu, Shear behaviour of architectural fabrics subjected to biaxial tensile loads, Composites Part A: Applied Science and Manufacturing (66) (2014) 163–174. doi:10.1016/j.compositesa.2014.07.015.

[6] M. Van Craenenbroeck, Biaxial Testing of Fabrics - Test methodologies and their impact on material parameters and the structural design process, Ph.D. thesis, Vrij Universiteit Brussel (2016).

[7] C. Galliot, R. H. Luchsinger, Determination of the response of coated fabrics under biaxial stress: Comparison between different test procedures, in: E. Oñate, B. Kröplin, K.-U. Bletzinger (Eds.), 5th International Conference on Textile Composites and Inflatable Structures, Structural Membranes 2011, 2011.

[8] B. N. Bridgens, P. D. Gosling, G.-T. Jou, X.-Y. Hsu, Inter-laboratory comparison of biaxial tests for architectural textiles, Journal of the Textile Institute 103 (7) (2012) 706–718. doi:10.1080/00405000.2011.602824.

[9] J. Uhlemann, Elastic Constants of Architectural Fabrics for Design Purposes, Ph.D. thesis, Universität Duisburg-Essen (2016).

[10] M. Van Craenenbroeck, M. Mollaert, L. De Laet, The influence of test conditions and mathematical assumptions on biaxial material parameters of fabrics, Engineering Structures (200) (2020). doi:10.1016/j.engstruct.2019.109691.

[11] L. Zhang, Reliability analysis of fabric structures, Ph.D. thesis, Newcastle University (2010).

[12] P. Gosling, B. Bridgens, L. Zhang, Adoptation of a reliability approach for membrane structure analysis, Structural Safety (40) (2013) 39–50. doi:10.1080/00405000.2011.602824.

[13] European Committee for Standardisation (CEN), EN 17117-1 Rubber or plastic-coated fabrics - Mechanical test methods under biaxial stress states - Part 1: Tensile stiffness properties (2018).

[14] Sioen Industries, T2103.pdf, `http://www.sioencoating.com/sites/default/files/T2103.pdf`, accessed: 09-03-2020.

[15] Allied Vision, Stingray F-504 High performance IEEE 1394b camera - 5 Megapixel - 9 fps, `https://www.alliedvision.com/en/products/cameras/detail/Stingray/F-504.html`, accessed: 09-03-2020.

[16] Correlated Solutions, Correlated Solutions - VIC-3D, `http://correlatedsolutions.com/vic-3d/`, accessed: 09-03-2020.

[17] B. N. Bridgens, Architectural fabric properties : determination , representation & prediction, Ph.D. thesis, Newcastle University (2005).

[18] P. Gosling, B. Bridgens, Material Testing & Computational Mechanics - A New Philosophy for Architectural Fabrics, Journal of Space Structures 23 (4) (2008) 215–232.

[19] Membrane Structures Association of Japan, Testing Method for Elastic Constants of Membrane Materials (MSAJ/M-02-1995), Tech. rep., Tokyo (1995).

[20] M. Van Craenenbroeck, L. De Laet, S. Puystiens, D. Van Hemelrijck, M. Mollaert, Biaxial testing of fabric materials and deriving their material properties – A quantitative study, in: Proceedings of the International Association for Shell and Spatial Structures (IASS) Symposium 2015, Amsterdam Future Visions, International Association for Shell and Spatial Structures (IASS), Amsterdam, 2015.

[21] The Mathworks, Inc., MATLAB - MathWorks - MATLAB & Simulink, `https://www.mathworks.com/products/matlab.html`, accessed: 09-03-2020.

[22] B. Bridgens, P. Gosling, Interpretation of results from the MSAJ "Testing method for elastic constants of membrane materials", in: Tensinet Symposium - Tensile Architecture: Connecting Past and Future, 2010, pp. 49–57.

[23] E. De Smedt, M. Mollaert, M. Van Craenenbroeck, R. Caspeele, L. Pyl, Reliability-based analysis of a cable-net structure designed using partial factors, in: Proceedings of the TensiNet Symposium 2019, 2019, pp. 316–326.

[24] H. W. Lilliefors, On the Kolmogorov-Smirnov Test for Normality with Mean and Variance Unknown, Journal of the American Statistical Association 62 (318) (1967) 399.

[25] W. Stute, W. Gonzáles-Manteiga, M. P. Quindimil, Bootstrap based goodness-of-fit tests, Metrika 40 (1993) 243–256.

[26] N. Mohd Razali, Y. Bee Wah, Comparisons of Shapiro-Wilk, Kolmogorov-Smirnov, Lilliefors and Anderson-Darling tests, Journal of Statistical Modeling and Analytics 2 (1) (2011) 21–33.